

Hole-state density of $\text{La}_{1-x}\text{Sr}_x\text{CoO}_{3-\delta}$ ($0 \leq x \leq 0.5$) across the insulator/metal phase boundary

A. R. Moodenbaugh and B. Nielsen

Department of Applied Science, Brookhaven National Laboratory, Upton, New York 11973-5000

Sharadha Sambasivan

National Synchrotron Light Source, Brookhaven National Laboratory, Upton, New York 11973-5000

D. A. Fischer

Materials Science and Engineering Laboratory, National Institute of Standards and Technology, Gaithersburg, Maryland 20899

T. Friessnegg, S. Aggarwal, and R. Ramesh
University of Maryland, College Park, Maryland 20742

R. L. Pfeffer

Serin Physics Laboratory, Rutgers, The State University, Piscataway, New Jersey 08854-8019

(Received 8 September 1999)

Oxygen K near-edge x-ray-absorption fine-structure (NEXAFS) of polycrystalline and film $\text{La}_{1-x}\text{Sr}_x\text{CoO}_{3-\delta}$ at room temperature was studied using fluorescence yield techniques. The bulk-sensitive nature of fluorescence yield (relative to electron yield), combined with the 0.2 eV incident photon resolution, allow us to accurately determine the evolution with x and δ of the oxygen K NEXAFS. For LaCoO_3 , a complex prepeak is centered near an energy $E=530.5$ eV. This peak, which has a full width at half maximum of about 3.0 eV, has been identified with oxygen bonding to Co $3d$ electrons. With Sr substitution we observe a distinct oxygen hole peak with an intensity proportional to x , centered near $E=528.8$ eV, with a full width at half maximum of 1.2 eV. In oxygen-reduced samples the hole peak tends to decrease in intensity as oxygen is removed. Comparisons are made with theoretical work and with earlier oxygen K near-edge studies on similar materials, most of which utilized electron yield. The behavior of the prepeak features with Sr (hole) doping parallels that observed in the oxide superconductors. Oxygen K NEXAFS of $\text{La}_{0.5}\text{Sr}_{0.5}\text{CoO}_{3-\delta}$ thin films is compared with bulk results to estimate relative oxygen contents of the films.

INTRODUCTION

The electronic structures of perovskites and related compounds are of interest for a variety of reasons. The high transition temperature (T_c) superconductors are layer perovskites, and have been investigated thoroughly. An impressive base of experimental and theoretical knowledge has been accumulated in the study of oxygen K near-edge x-ray-absorption fine structure (NEXAFS) of these materials.¹ More recently, perovskite oxides similar to those in the present study (most notably $\text{La}_{1-x}\text{Ca}_x\text{MnO}_3$) have been the subject of intense study because of their interesting fundamental electronic and magnetic properties, as well as a variety of potential applications, especially those related to magnetoresistance effects. The perovskite $\text{La}_{1-x}\text{Sr}_x\text{CoO}_3$ is also of technological interest, based on electronic and ionic conductivity. There is an insulator/metal phase boundary at room temperature near Sr $x=0.2$. $\text{La}_{1-x}\text{Sr}_x\text{CoO}_3$ is a candidate material for use as a cathode in solid oxide fuel cells² and as an oxygen-permeable membrane.³ In the development of metal-oxide-based device technologies, the electrically conductive composition $\text{La}_{0.5}\text{Sr}_{0.5}\text{CoO}_{3-\delta}$ is finding application as an electrode material. The reliability of ferroelectric memory cells based on $\text{Pb}(\text{Zr},\text{Ti})\text{O}_3$ is significantly improved by replacing the typical Pt electrodes with $\text{La}_{0.5}\text{Sr}_{0.5}\text{CoO}_{3-\delta}$.⁴

We investigated the electronic structure of bulk and film $\text{La}_{1-x}\text{Sr}_x\text{CoO}_3$ using oxygen K NEXAFS. In the high- T_c superconductors, the oxygen K NEXAFS prepeaks have been interpreted in terms of a Hubbard band with a charge-transfer model of hole creation.⁵ In an undoped material, La_2CuO_4 for example, a small peak appears on the leading part of the oxygen K edge, just above the Fermi level, near 531 eV. This feature is attributed to the oxygen hybridizing to Cu d electrons, and is called the d -band, or hybridization, peak.⁶ With hole doping (Sr $x>0$) this peak decreases in size, while another peak appears near the Fermi level (529 eV) due to hole states with oxygen character (hole peak).⁶

Abbate *et al.*,⁷ based on soft-x-ray studies of the transition-metal edges, suggested that holes introduced into the system may either be accommodated in a transition-metal state (in cases when an ion, V^{3+} or Mn^{3+} for example, can be further ionized) or as an oxygen hole state (in Cu, for example, where Cu^{3+} is not as easily attainable). This same group⁸ later compared the $\text{La}_{1-x}\text{Sr}_x\text{FeO}_3$ and $\text{La}_{1-x}\text{Sr}_x\text{MnO}_3$ oxygen near edges to illustrate the distinct character difference between the added oxygen hole state and a hole with primarily transition-metal character. With Sr substitution into the Fe perovskite, a relatively narrow prepeak develops on the oxygen K near edge, indicating an oxygen hole state. In the Sr-substituted Mn perovskite, no such sharp prepeak occurs, the additional electronic states being associated prima-

rily with the Mn d band. There are strong similarities between the well-documented oxygen K NEXAFS of high- T_c materials and that of $\text{La}_{1-x}\text{Sr}_x\text{CoO}_3$. The electronic states introduced into $\text{La}_{1-x}\text{Sr}_x\text{CoO}_3$ by substituting Sr^{2+} for La^{3+} are oxygen holes, as in $\text{La}_{2-x}\text{Sr}_x\text{CoO}_4$, not states primarily associated with the Co $3d$ band.

The system $\text{La}_{1-x}\text{Sr}_x\text{CoO}_3$ has several interesting electronic and magnetic features. In LaCoO_3 itself there is a change in Co from low to intermediate spin state near 100 K. Well above room temperature, an insulator to metal transition is associated with an intermediate to high-spin transition.⁹ In $\text{La}_{1-x}\text{Sr}_x\text{CoO}_3$ at room temperature, there is an insulator-metal phase boundary, with metallic conductivity for $x > 0.2$.¹⁰

These materials are slightly distorted from cubic to rhombohedral symmetry, with the rhombohedral angle $\alpha = 60.8^\circ$ at $x = 0$ falling to $\alpha = 60.2^\circ$ at $x = 0.5$. However, in bulk randomly oriented polycrystalline samples we cannot observe differences due to departure from cubic symmetry. There has been an effort to calculate the oxygen K near-edge spectrum in this system, taking into account the departure from cubic symmetry which shows small differences.¹¹ For the films (compositions at Sr $x = 0.5$ where the rhombohedral distortion is very slight), we will neglect direction dependent effects.

Most earlier oxygen K NEXAFS studies of $\text{La}_{1-x}\text{Sr}_x\text{CoO}_3$ were done using the electron yield method. Abbate *et al.*¹² studied the temperature (T) dependence of the oxygen K near edge in a single crystal LaCoO_3 using partial electron yield, with about 0.13-eV resolution. They observed a feature on the leading edge of the hybridization peak developing well above room temperature. They attributed this to the low-to-intermediate-spin-state transition, even though convincing evidence shows the transition to occur near 100 K.^{9,13} Sarma *et al.*¹⁴ used fluorescence yield in a survey of the oxygen K near edges at room temperature in a series of perovskite oxides. Their results for LaCoO_3 are comparable to those obtained in the present study.

Sarma *et al.*¹⁵ used total electron yield to study the oxygen K NEXAFS in $\text{La}_{1-x}\text{Sr}_x\text{CoO}_3$ with Sr $x \leq 0.3$, at a resolution of 0.7 eV. These authors observed a large increase in the intensity near the $E = 530$ eV with x , which they attributed to hole states. The broad feature identified as a hole peak might suggest, according to the reasoning of Abbate co-workers,^{7,8} that in this system the holes are primarily of Co $3d$ character.

In this work the combination of high resolution in incident photon energy, 0.2 eV, with bulk sensitivity provides reliable data on which we base a more detailed analysis. The electron yield method is quite sensitive to surface conditions. The total electron yield data of Sarma *et al.*¹⁵ on $\text{La}_{1-x}\text{Sr}_x\text{CoO}_3$ may have been affected by surface contamination. For LaCoO_3 , partial yield data on a single crystal¹² as well as the earlier fluorescence yield results¹⁴ appear to correspond well to the present fluorescence yield data at room temperature.

The measurement of the oxygen K NEXAFS of the $\text{La}_{0.5}\text{Sr}_{0.5}\text{CoO}_{3-\delta}$ films provides information on relative oxygen contents not previously available, to our knowledge. Electrical properties are strongly influenced by oxygen non-stoichiometry δ , which depends on doping level and process-

ing conditions such as oxygen partial pressure. Cooling from process temperature in a reducing atmosphere of Pb-based ferroelectric thin-film capacitors with $\text{La}_{0.5}\text{Sr}_{0.5}\text{CoO}_{3-\delta}$ electrodes results in an increased tendency to imprint failure, whereas fully oxidized capacitors exhibit no imprint.¹⁶ This effect is related to defects in the electrode layers, the defects being associated with oxygen deficiency. Oxygen-vacancy-related defects have been detected in these films using positron annihilation spectroscopy.¹⁷ The NEXAFS hole peak intensities of films prepared under a variety of conditions are compared with the hole peak intensities of bulk samples whose oxygen contents are known. We use these results to estimate the oxygen contents of $\text{La}_{0.5}\text{Sr}_{0.5}\text{CoO}_{3-\delta}$ films.

EXPERIMENT

Samples nominally $\text{La}_{1-x}\text{Sr}_x\text{CoO}_3$, Sr $x = 0, 0.10, 0.18, 0.25, 0.3, \text{ and } 0.5$, were prepared in air similar to previously published methods.¹⁸ Final cooling of the samples was at 100 °C per day in air to maximize oxygen contents. Oxygen contents of the bulk samples can be estimated by indirect methods. Earlier literature suggests that the oxygen content of samples prepared in air $0 \leq x \leq 0.5$ are near stoichiometric when slow cooled in air.¹⁹ We attach a nominal oxygen formula content of 3 to all our bulk samples, but acknowledge the possibility of a departure from this value. Oxygen-reduced samples were made by quenching from 1100 °C in air to liquid nitrogen. The change in oxygen content was estimated by following the mass of the sample. The difference in mass was attributed to a change in oxygen, and from this we calculated a nominal oxygen content assuming 3 as the initial value. Nominal reductions in oxygen content are, for $x = 0.10, \delta = 0.03$ and, for $x = 0.50, \delta = 0.29$. Before being introduced into the vacuum chamber for measurement, samples were lightly sanded.

Thin films of $\text{La}_{0.5}\text{Sr}_{0.5}\text{CoO}_{3-\delta}$ were grown on LaAlO_3 substrates by pulsed excimer laser deposition using a solid ceramic target of the same composition. During deposition, a temperature of 650 °C and a pressure of 100-mTorr oxygen were maintained in the growth chamber. After growth, the films (labeled Nos. 1, 2, and 3) were cooled at 5 °C/min in varying oxygen partial pressures, in Torr, of 10^{-1} , 10^{-2} , and 10^{-3} , respectively. The phase purity and structural quality of the films were evaluated by x-ray diffraction, showing epitaxial growth.

The NEXAFS experiments were performed at the soft-x-ray beamline U7A of the National Synchrotron Light Source at Brookhaven National Lab. Fluorescence yield data were obtained for the oxygen K edges, with electron yield data collected simultaneously for most samples.²⁰ The energy resolution of the incident photons is 0.2 eV.

The data for bulk samples were analyzed analytically using the following procedures. The data were first normalized to I_0 , the photon yield from a clean gold grid intercepting the incident beam. Then the pre-edge intensity was subtracted from the data, and the data were further normalized to an edge jump of unity, based on the observed intensity about 50 eV above the edge. In order to isolate the Co $3d$ hybridization peak (centered near 530.5 eV) and oxygen hole peak feature (528.8 eV) from the main edge, the fluorescence yield data were analyzed further. A Gaussian of fixed posi-

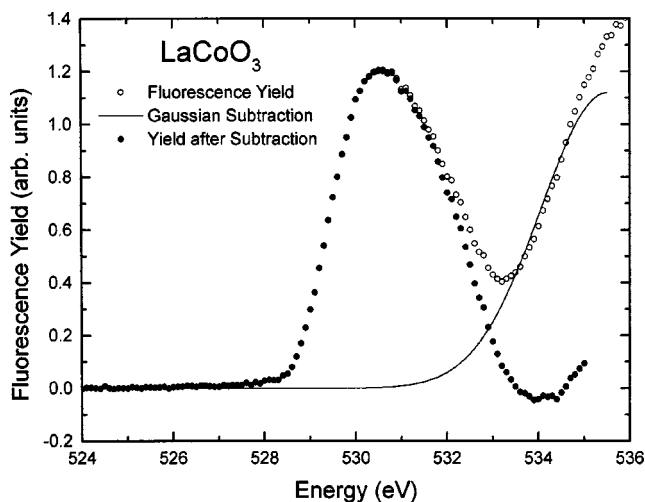


FIG. 1. Oxygen K near-edge region for bulk LaCoO_3 . Illustrated is the method used to isolate the prepeaks. A Gaussian with fixed position (535.5-eV center) and width (full width at half maximum of 1.45 eV), with amplitude fit to the main edge profile, is subtracted. The resulting isolated prepeak (assumed to be the hybridization peak for $x=0$) is shown as filled symbols.

tion (535.5 eV) and full width (2.45 eV), but with adjusted intensity, was subtracted from the main edge (see Fig. 1 for the case of $x=0$). The $x=0$ data was assumed to be purely due to the hybridization (Co $3d$ band) scattering. In order to make an estimate of the relative intensities of the hole peak and the $3d$ peak for $x>0$, the preferred procedure would be to fit the peaks analytically. However, the hybridization peak has a complicated shape, with the overall intensity of this peak decreasing with Sr x . Therefore, we chose to subtract a fraction of the $x=0$ hybridization peak in order to isolate the hole peak. For fully oxidized samples, the subtraction was made systematically with the hybridization peak intensity assumed to be proportional to $1-x/2$. Some changes in the shape of the hybridization peak occur with Sr substitution x , but we did not attempt to adjust for these changes. For reduced samples we made a visual estimate of the hybridization peak intensity to be subtracted. We then estimated intensities of the hole and d -band contributions to the NEXAFS based on the integrated intensities.

The film samples were analyzed similarly. The oxygen K NEXAFS of a bare substrate of LaAlO_3 was also obtained to compare to film results. No obvious LaAlO_3 component was observed in any of the samples. The relative oxygen content could then be estimated relative to the bulk samples based on the observed intensity of the oxygen hole peak.

RESULTS

Bulk $\text{La}_{1-x}\text{Sr}_x\text{CoO}_{3-\delta}$

Oxygen K NEXAFS from fluorescence yield for bulk $\text{La}_{1-x}\text{Sr}_x\text{CoO}_{3-\delta}$ shows a perceptible change with x (see Fig. 2). As Sr is substituted into the system, a well-defined peak at 528.8 eV grows in intensity with x . There is a simultaneous reduction in intensity of the hybridization peak centered near 530.5 eV. Other edge features change subtly. The

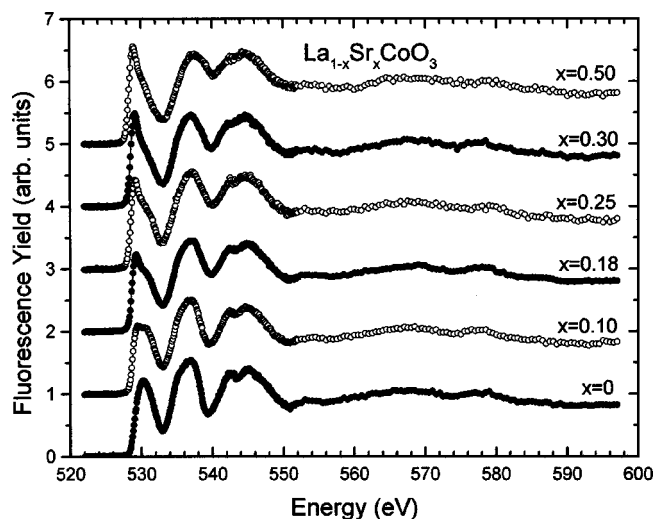


FIG. 2. Oxygen K near edges for bulk $\text{La}_{1-x}\text{Sr}_x\text{CoO}_3$ in fluorescence yield. Data have been normalized to edge jump, taken to be the difference in fluorescence yield from below the edge (near 522 eV) and well above the edge (570–580 eV). Curves are offset vertically for clarity.

double-peaked feature near 545 eV, identified with bonding to Co $4sp$ states,¹² becomes smeared out as Sr is substituted for La. The feature centered near 536 eV, due to La $5d$ bonding,¹² changes little with Sr substitution. Similar trends are qualitatively evident in the electron yield data (see Fig. 3), including the development of a well-defined hole prepeak near 528.8 eV.

Further analysis of the oxygen K NEXAFS quantifies some of these observations. Figure 1 shows the first step in the analysis, the isolation of the hybridization peak from the La $5d$ feature for $x=0$, by subtraction of a Gaussian approximation to the leading edge of the La $5d$ feature from the data. Figure 4 shows the hole peaks for all x 's after an estimated hybridization peak was subtracted, as described in the experimental section. A systematic increase in the intensity of the hole peak with x is readily apparent in Fig. 4. In

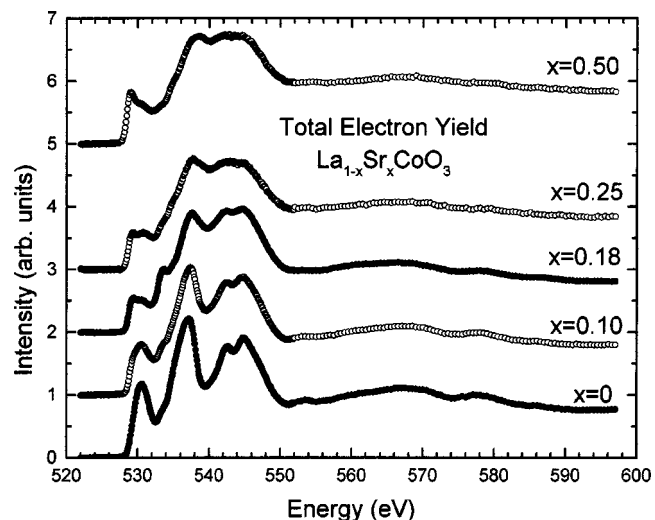


FIG. 3. Oxygen K near edges for bulk $\text{La}_{1-x}\text{Sr}_x\text{CoO}_3$ in electron yield. Data have been processed as was the fluorescence yield data in Fig. 2. Curves are offset vertically for clarity.

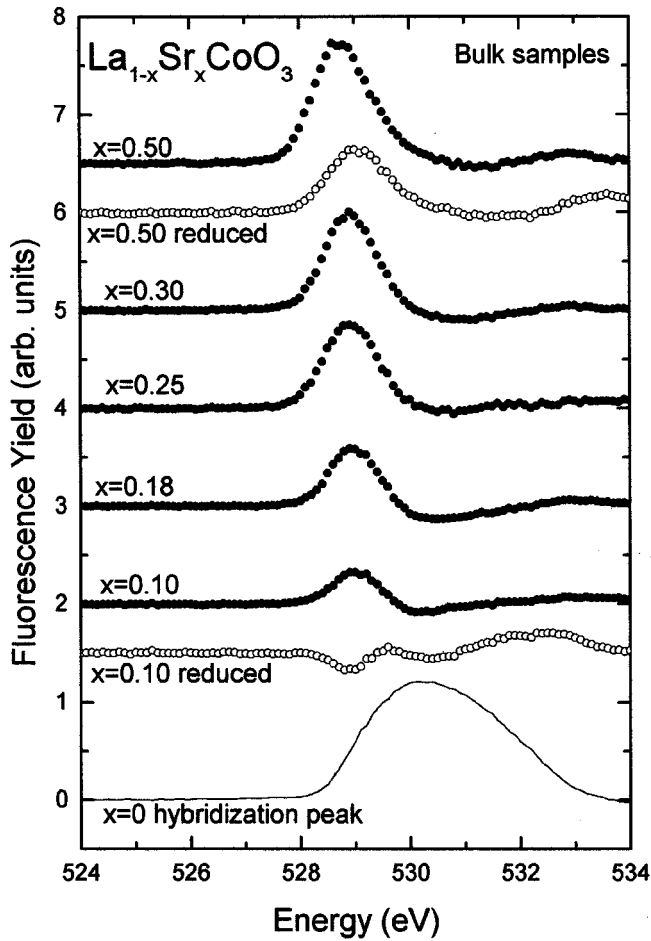


FIG. 4. Plot of the oxygen *K* hole peaks in bulk $\text{La}_{1-x}\text{Sr}_x\text{CoO}_{3-\delta}$ after subtraction of a fraction of the $x=0$ hybridization peak (illustrated at the bottom). Curves are offset vertically for clarity.

Fig. 4 near $E=531-3$ eV, the departure of the data from zero suggests there are some changes in the Co *3d* peak shape with Sr doping.

Figure 5 shows the relative intensities of the oxygen hole and hybridization peaks with Sr content x . The oxygen hole peak intensities are nearly linear, increasing with x out to $x=0.5$. Across the $x=0.2$ insulator/metal phase boundary, there appears to be a slight increase in the hole density over and above the nearly linear slope. The relative intensities for the corresponding peaks of reduced samples are shown as squares, also in Fig. 5. For both $x=0.10$ and 0.50 sizable changes in the hole peak intensities are observed, lower intensities being due to reduced hole densities. For the $x=0.10$ peak, the apparent hole peak intensity is less than zero. This suggests that there may be some residual oxygen hole character in the LaCoO_3 sample which, in order to analyze our data, we have assumed to be a Co *3d*-related intensity.

$\text{La}_{0.5}\text{Sr}_{0.5}\text{CoO}_{3-\delta}$ films

In this work we compare the bulk results with the film results, with the goal of estimating the oxygen content of the films. The oxygen hole prepeaks for the films are shown in Fig. 6, with the data for bulk Sr $x=0.50$ oxidized (nominal

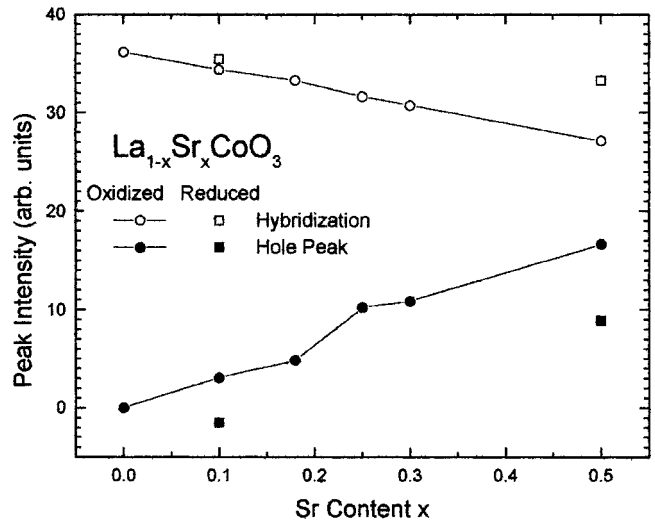


FIG. 5. Peak intensities from the analysis of the prepeaks in bulk oxidized $\text{La}_{1-x}\text{Sr}_x\text{CoO}_3$ (circles) and reduced $\text{La}_{1-x}\text{Sr}_x\text{CoO}_{3-\delta}$ (squares). The hybridization peak intensity for oxidized samples is linear in x because of assumptions made in the analysis. The hole peak intensities show an approximately linear dependence on x out to $x=0.5$. The reduced samples $x=0.1$ and 0.5 show an expected reduced hole peak intensity compared to the oxidized samples.

oxygen $\delta=0$) and reduced ($\delta=0.29$) samples replotted for comparison. The intensities of all the hole peaks were ob-

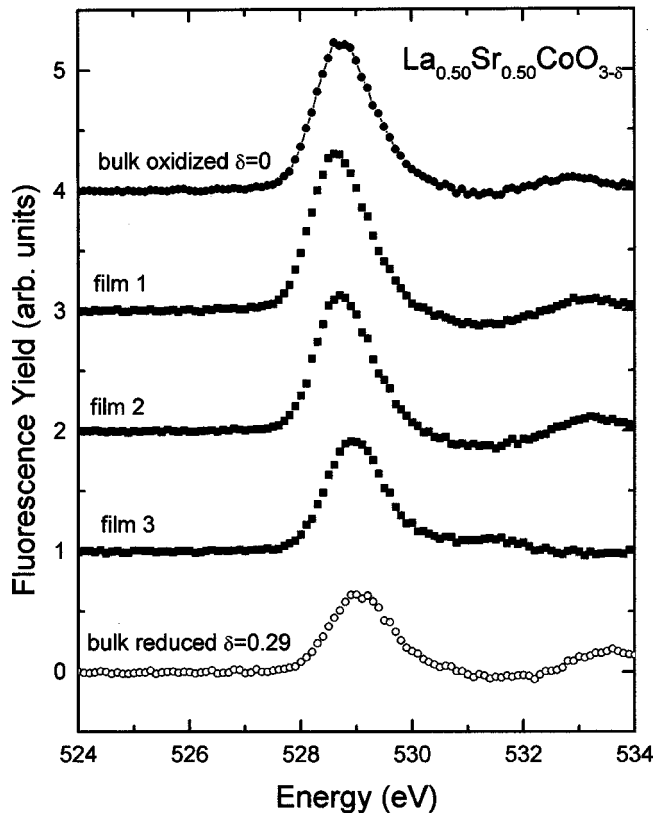


FIG. 6. Plot of the oxygen *K* hole peaks in film $\text{La}_{0.5}\text{Sr}_{0.5}\text{CoO}_{3-\delta}$ after subtraction of a fraction of the $x=0$ hybridization peak (illustrated at the bottom of Fig. 4). For comparison, the bulk oxidized and reduced Sr $x=0.50$ samples are replotted from Fig. 4. Curves are offset vertically for clarity.

TABLE I. Oxygen content estimates derived from oxygen K NEXAFS as described in the text. Sample cooling condition is the atmosphere in which the sample was cooled from reaction temperature.

Sample ID	Sample cooling conditions	Nom. oxygen from NEXAFS
1	10^{-1} -Torr O_2	3.01
2	10^{-2} -Torr O_2	2.87
3	10^{-3} -Torr O_2	2.79

tained by integrating the peak area. We estimate the oxygen contents of the film samples using the bulk samples as a standard, after making some reasonable assumptions. First, we assume a linear relation between oxygen content and integrated intensity for the bulk hole peak. Second, we assume that the film hole peak intensities are not materially affected by the slight distortion from cubic structure. The resulting estimated oxygen contents from EXAFS are shown in Table I. The source of most of the uncertainties entering into these values stems from systematic errors introduced during the edge subtraction process, where slight changes in overlapping peak shapes or unaccounted for shifts in energy scale might affect the value by up to ± 0.05 in oxygen content. The estimated oxygen contents derived from the NEXAFS measurements are qualitatively reasonable, based on the cooling conditions.

DISCUSSION

First we compare the present fluorescence yield results for bulk $La_{1-x}Sr_xCoO_3$ with those of Sarma *et al.* using electron yield.¹⁵ Those authors showed a much larger growth in intensity with Sr x near the hole peak than our data indicate. The combined intensity of their hybridization and hole peaks nearly doubled from $x=0$ to 0.2. They attributed the increase to the development of a broad hole peak. Using fluorescence yield we observe a much smaller increase in total prepeak intensity with Sr x as well as a significantly sharper peak (1.2-eV full width at half maximum) By summing the hole and hybridization peak intensities plotted in Fig. 5, we can estimate the change in our prepeak total intensities. We observe a total increase of only about 20% between $x=0$ and 0.5. For comparison we recorded electron yield simultaneously with fluorescence yield for most of these samples. The net intensity of the pre-edge features (528–531 eV) in our electron yield (see Fig. 3) actually *decreases* with x , even though for $x=0$ our electron yield data are in reasonable agreement with those of Sarma *et al.* At the same time, in our electron yield results, the development of a well-defined oxygen hole peak near 529 eV for $x>0$ is apparent. We feel that the surface sensitivity of the electron yield method makes any quantitative conclusions arising from either set of electron yield results problematic. Another possible source of the systematic discrepancy may be that the two sets of data were normalized differently. As with high- T_c superconductors, fluorescence yield provides more reliable data on bulk properties. Our well-defined hole peak, seen in both fluorescence and

electron yield, is characteristic of holes with primarily oxygen character, as observed in the layer perovskite oxides.

The temperature dependence of the near edge of $LaCoO_3$ using partial electron yield illustrates many interesting features. Abbate *et al.*¹² displayed electron yield data on a single-crystal sample which corresponds fairly well to the fluorescence yield data of the present study. Their room-temperature (and below) data showed a peak qualitatively similar to our $x=0$ data. Those authors suggested that above room temperature, based on a theoretical analysis, a second prepeak on the leading edge of the d -band peak, near 529 eV, is due to a repopulation of the d orbitals, the low to intermediate spin transition. However, it has been shown fairly conclusively that the so-called d -band repopulation occurs near $T=100$ K.^{9,13,21} We suggest that this observed high-temperature prepeak is likely a hole peak appearing near the temperature that metallic conduction appears in $LaCoO_3$.

To our knowledge, the present results are the first fluorescence yield data for $La_{1-x}Sr_xCoO_3$ ($x>0$), providing systematic data representative of the bulk. The 0.2-eV incident photon resolution of the present study allows a better analysis of the oxygen K prepeak region in the $La_{1-x}Sr_xCoO_3$ than previously available. A prepeak feature near 528.8 identified as the oxygen hole peak is similar to that observed in the oxide superconductors, and has an intensity proportional to nominal hole doping (here Sr x). The broad peak centered near 530.5 eV attributed to Co $3d$ bonding (hybridization peak) is relatively more intense than a similar Cu $3d$ hybridization peak in the oxide superconductors. But like the Cu peak, the Co $3d$ peak decreases smoothly in intensity with hole doping. There may be a slight increase in the oxygen K NEXAFS hole peak intensity (Fig. 5) across the insulator/metal boundary near $x=0.2$. This would be an interesting feature not evident in the cuprates, which needs to be confirmed by additional measurements.

The oxygen K NEXAFS study of $La_{0.5}Sr_{0.5}CoO_{3-\delta}$ films provides a basis for estimating oxygen content in the films. The results shown in Table I suggest that basic trends in oxygen content can be monitored by this method. However, reproducibility and accuracy are not well understood. Reliability could be better assessed by comparing a more comprehensive set of results, as well as comparing results from independent techniques.

ACKNOWLEDGMENTS

Research at Brookhaven was supported by the U.S. Department of Energy, Office of Basic Energy Sciences, Division of Materials Sciences, under Contract No. DE-AC02-98CH10886. The National Synchrotron Light Source is supported by the U.S. Department of Energy, Divisions of Materials Sciences and Chemical Sciences. This work was also funded by the Army Research Laboratory under Cooperative Agreement No. DAAL01-95-2-3530.

- ¹ For a review, see J. Fink, N. Nucker, E. Pellegrin, H. Romberg, M. Alexander, and M. Knupfer, *J. Electron Spectrosc. Relat. Phenom.* **66**, 395 (1994).
- ² Y. Kaga, Y. Ohno, K. Tsukamoto, F. Uchiyama, M. J. Lain, and T. Nakajima, *Solid State Ionics* **40–41**, 1000 (1990).
- ³ Y. Teraoka, H. Zhang, S. Furukawa, and N. Yamazoe, *Chem. Lett.* **1985**, 1743 (1985).
- ⁴ R. Ramesh, H. Gilchrist, T. Sands, V. G. Keramidas, R. Haakenaasen, and D. K. Fork, *Appl. Phys. Lett.* **63**, 3592 (1993).
- ⁵ H. Eskes, M. B. J. Meinders, and G. A. Sawatzky, *Phys. Rev. Lett.* **67**, 1035 (1991).
- ⁶ C. T. Chen, F. Sette, Y. Ma, M. S. Hybertsen, E. B. Stechel, W. M. C. Foulkes, M. Schluter, S.-W. Cheong, A. S. Cooper, L. W. Rupp, B. Battlogg, Y. L. Soo, Z. H. Ming, A. Krol, and Y. H. Kao, *Phys. Rev. Lett.* **66**, 104 (1991).
- ⁷ M. Abbate, F. M. F. de Groot, J. C. Fuggle, A. Fujimori, Y. Tokura, Y. Fujishima, O. Strebel, M. Domke, G. Kaindl, J. van Elp, B. T. Thole, G. A. Sawatzky, M. Sacchi, and N. Tsuda, *Phys. Rev. B* **44**, 5419 (1991).
- ⁸ M. Abbate, F. M. F. de Groot, J. C. Fuggle, A. Fujimori, O. Strebel, F. Lopez, M. Domke, G. Kaindl, G. A. Sawatzky, M. Takano, Y. Takeda, H. Eisaki, and S. Uchida, *Phys. Rev. B* **46**, 4511 (1992).
- ⁹ M. A. Senaris-Rodriguez and J. B. Goodenough, *J. Solid State Chem.* **116**, 224 (1995).
- ¹⁰ M. A. Senaris-Rodriguez and J. B. Goodenough, *J. Solid State Chem.* **118**, 323 (1995).
- ¹¹ Z. Y. Wu, M. Benfatto, M. Pedio, R. Cimino, S. Mobilio, S. R. Barman, K. Maiti, and D. D. Sarma, *Phys. Rev. B* **56**, 2228 (1997).
- ¹² M. Abbate, J. C. Fuggle, A. Fujimori, L. H. Tjeng, C. T. Chen, R. Potze, G. A. Sawatzky, H. Eisaki, and S. Uchida, *Phys. Rev. B* **47**, 16 124 (1993).
- ¹³ K. Asai, O. Yokokura, N. Nishimori, H. Chou, J. M. Tranquada, G. Shirane, S. Higuchi, Y. Kajima, and K. Kohn, *Phys. Rev. B* **50**, 3025 (1994).
- ¹⁴ D. D. Sarma, O. Rader, T. Kachel, A. Chainani, M. Mathew, K. Holdack, W. Gudat, and W. Eberhardt, *Phys. Rev. B* **49**, 14 238 (1994).
- ¹⁵ D. D. Sarma, A. Chainani, R. Cimono, P. Sen, C. Carbone, M. Mathew, and W. Gudat, *Europhys. Lett.* **19**, 513 (1992).
- ¹⁶ S. Aggarwal, A. M. Dhote, R. Ramesh, W. L. Warren, G. E. Pike, D. Dimos, M. V. Raymond, and J. T. Evans, Jr., *Appl. Phys. Lett.* **69**, 2540 (1996).
- ¹⁷ D. J. Keeble, A. Krishnan, T. Friessnegg, B. Nielsen, S. Mahukar, S. Aggarwal, R. Ramesh, and E. H. Poindexter, *Appl. Phys. Lett.* **73**, 508 (1998).
- ¹⁸ V. Golovanov, L. Mihaly, and A. R. Moodenbaugh, *Phys. Rev. B* **53**, 8207 (1996).
- ¹⁹ J. Mizusaki, Y. Mima, S. Yamauchi, and K. Fueki, *J. Solid State Chem.* **80**, 102 (1989).
- ²⁰ D. A. Fischer, J. Colbert, and J. L. Gland, *Rev. Sci. Instrum.* **60**, 2596 (1989).
- ²¹ R. Caciuffo, D. Rinaldi, G. Barucca, J. Mira, J. Rivas, M. A. Senaris-Rodriguez, P. G. Radaelli, D. Fiorani, and J. B. Goodenough, *Phys. Rev. B* **59**, 1068 (1999).